

Macroseismic effects highlight site response in Rome and its geological signature

Paola Sbarra^{a)}, Valerio De Rubeis^{a)}, Emiliano Di Luzio^{b)}, Marco Mancini^{c)}, Massimiliano Moscatelli^{c)}, Francesco Stigliano^{c)}, Patrizia Tosi^{a)} and Roberto Vallone^{c)}

a) *Istituto Nazionale di Geofisica e Vulcanologia, Roma, Via di Vigna Murata, 605 Roma, Italy 00143*

b) *Istituto per le Tecnologie Applicate ai Beni Culturali (ITABC). Consiglio Nazionale delle Ricerche Area della Ricerca Roma RMI –Montelibretti, Via Salaria km 29.300, Monterotondo Stazione – Roma, Italy C.P. 10 - 00015*

c) *Istituto di Geologia Ambientale e Geoingegneria (IGAG). Consiglio Nazionale delle Ricerche Area della Ricerca di Roma RM 1 – Montelibretti, Via Salaria km 29.300, Monterotondo Stazione – Roma, Italy C.P. 10 – 00015*

The final publication is available at springerlink.com

Corresponding (first) author: Paola Sbarra

Phone: +39 0651860276

Fax: +39 065041181

Mailing address: paola.sbarra@ingv.it

ABSTRACT

A detailed analysis of the earthquake effects on the urban area of Rome has been conducted for the L'Aquila sequence, which occurred in April 2009, by using an on-line macroseismic questionnaire. Intensity residuals calculated using the mainshock and four aftershocks are analyzed in the light of a very accurate and original geological reconstruction of the subsoil of Rome based on a large amount of wells. The aim of this work is to highlight ground motion amplification areas and to find a correlation with the geological settings at a sub-regional scale, putting in evidence the extreme complexity of the phenomenon and the difficulty of making a simplified model. Correlations between amplification areas and both near-surface and deep geology were found. Moreover, the detailed scale of investigation has permitted us to find a correlation between seismic amplification in recent alluvial settings and subsiding zones, and between heard seismic sound and Tiber alluvial sediments.

KEYWORDS

Earthquakes, Intensity residuals, Urban geosciences, Macroseismic effects, Amplification areas.

INTRODUCTION

Human response to ground shaking, when averaged over a large number of samples, is a very good indicator of the level of ground motion (Kayano, 1990; Dengler and Dewey, 1998). People and buildings can be considered as “instruments” in recording seismic effects such as shaking intensity, movements of objects, human reactions and damage. The use of web-based macroseismic surveys to record this information has grown significantly with the wide diffusion of Internet connections. It presents several positive features, such as: almost real-time results, low-cost surveys, fast evaluation of earthquake severity, and positive feedback between seismic institutions and people. In

addition, a large amount of data, which is available even for very small events, allows for statistical evaluation of intensities.

In April 2009, a seismic sequence occurred in central Italy, near the town of L'Aquila. More than 300 people lost their lives (over a total population of 66,813) because of the collapse of buildings during the mainshock, which had a magnitude of $M_I=5.8$. The mainshock in the epicentral area reached VIII-IX Mercalli-Cancani-Sieberg (MCS) intensity (Sieberg, 1930) and the most relevant damage was distributed in the NW-SE direction, with predominance toward the southeast (Fig. 1a). In the days following there were four major aftershocks (Tab. 1), which were felt in the entire area of central Italy (Fig. 1). A detailed macroseismic analysis was conducted in Rome, where a large amount of data was collected from web-compiled questionnaires (3,695 reliable questionnaires). The data regard low-intensity degrees, characterized mostly by transient effects recorded by people all over the urban area, which is located at a distance of around 90 km from the city of L'Aquila (Fig. 2a).

In order to evaluate seismic hazard and site effects, the correct evaluation of seismic waves amplification due to differences in outcropping lithology and local geological settings is necessary (Seekins and Boatwright, 1994; Bakir et al., 2002; Semblat et al., 2002; Pergalani et al., 2006; Lee et al., 2009). Macroseismic data in urban areas have already been used to identify amplification zones (Sousa and Oliveira, 1997; Toshinawa, 1997; Giammarinaro et al., 2005; Panou et al., 2005; Ocola, 2008; Carlino et al., 2009). Although Rome is settled in a relatively low-seismicity area, it has suffered damage produced by earthquakes in the past, the sources of which were mainly located in the Albani Hills and in the central Apennines. In this regard, previous works dealing with the macroseismicity of Rome, such as Ambrosini et al. (1986) and Molin and Guidoboni (1989), have assessed different levels of damage caused by historical earthquakes, and found a correlation between amplification areas and surface geology. In particular, these studies have shown an amplification in correspondence to the Tiber River alluvial deposits inside the historical centre of Rome. The same conclusions were obtained by Tertulliani et al. (1996), Cifelli et al. (2000) and Donati et al. (2008), regarding recent events that did not produce damage; these authors, indeed, also observed an amplification in the Tiber valley outside of the historical center and in the Aniene River valley. As a matter of fact, Rome has been affected by intense urbanization in peripheral neighborhoods during the last 50 years, which has increased the importance of detecting seismic intensity amplification in the new expanding zones. Our work confirms the seismic amplification in some of these zones. Moreover, due to the great detail of both seismic local intensity data and geological setting analysis carried on independently, we are able to put in evidence, for the first time, the important role of deep geology in the macroseismic behavior of Rome.

GEOLOGICAL SETTING

The geological setting presented in this paper was elaborated by the Istituto di Geologia Ambientale e Geoingegneria (IGAG) of the Consiglio Nazionale delle Ricerche (CNR), using more than 6,000 stratigraphic and geotechnical boreholes as a part of the UrbiSIT Project (Fig. 2).

Rome stands on a hilly area located in the piedmont region lying at the west of the central Apennines, close to the Tyrrhenian Sea coastline (Figs. 3, 2a). The area is crossed by the Tiber and Aniene Rivers, flowing from N to S and from E to W, respectively, which are bordered by narrow alluvial plains. On the right bank (westward) of the Tiber River, the landscape is dominated by NW-SE and N-S elongated ridges, up to 140 m a.s.l. in elevation. On the left bank (eastward), a wide tabular plateau of distal volcanites stands at 50-60 m a.s.l., laterally continuous with the gentle north-western flank of the Albani Hills.

The geological substratum of the city is characterized by Pliocene-Lower Pleistocene marine sedimentary deposits (MMV unit in Fig. 2) covering underlying Mesozoic-Cenozoic carbonate and terrigenous successions with angular unconformity (Funicciello et al., 2008 and references therein). Plio-Pleistocene units are covered by continental deposits, late Early Pleistocene-Holocene in age, interbedded with products from the Sabatini Mountains and Albani Hills Volcanic Districts (Fig. 2). In the last 3,000 years, anthropic activities have modified the original geomorphology of the countryside (Funicciello et al., 2008 and references therein), now hidden by man-made deposits (AB unit in Fig. 2).

The structural style of the study area is dominated by alternating horsts and grabens formed during the Pliocene-Early Pleistocene time interval and bounded by NW-SE oriented normal faults. Such structures are locally dissected by NE-SW trending transverse faults. This main arrangement is complicated by a younger (Early-Middle Pleistocene) N-S oriented fault system in the central-western part of the city (Fig. 2a). All of these features are superimposed on previous compressional NW-SE trending fold and thrust structures, involving pre-Pliocene successions (Funicciello et al., 2008).

As aforementioned, the regional substratum is composed of marine, overconsolidated clays and sands of the Pliocene-Early Pleistocene age (MMV unit, which comprises the Monte Vaticano and Monte Mario Formations according to Funicciello et al., 2008), and reaches a maximum thickness of about 900 m in the centre of Rome (Circo Massimo exploration well; Signorini, 1939). A late Early Pleistocene-Holocene continental geological multilayer including both sedimentary deposits and Middle-Upper Pleistocene volcanites, unconformably covers the Pliocene-Early Pleistocene marine substratum. This upper complex is composed, from bottom to top, of three main informal stratigraphic units, which are described below.

1) Continental deposits of the “Paleotiber unit” (PT unit in Fig. 2, late Early-Middle Pleistocene; see Marra et al., 1998), which include several fining upward, decameter thick and vertically stacked depositional cycles. These cycles is characterized, in general, by basal fluvial gravels and sands passing over fluvio-lacustrine pelites, locally rich in organic matter. The cycles are stacked to form an approximately 150-m thick basin-fill, within the NW-SE oriented tectonic depression of the Paleotiber Graben (Figs. 2b, 2c). In this graben, the gravelly-sandy layers and the pelitic intervals are regularly alternated and are almost in equal vertical proportion (see also Florindo et al. 2007).

Conversely, in the area of the historical city centre, the PT unit is much thinner (few tens of meters to less than 10 m) than in the Paleotiber Graben (Figs. 2b, 2c), and is composed at most of gravels and sands, only referable to two depositional cycles (Paleotiber 2a and 2b, Marra et al., 1998)

The “Paleotiber unit” in this work also includes lagoonal and fluvio-deltaic deposits of the Ponte Galeria Formation, which is located between the south-western part of the city and the Tyrrhenian Sea coastline (Milli, 1997, and references therein).

2) A wide and thick volcanic unit (VT unit in Fig. 2; Middle-Late Pleistocene), is characterized by pyroclastic deposits locally interbedded with lavas and sedimentary layers. Volcanics were emitted between 600 and 30 ka from the nearby Sabatini Mountains and Albani Hills Volcanic Districts. They are mostly represented by: i) deposits related to thick and wide pyroclastic flows, composed of lithic tuffs, ignimbrites and welded ashes with interbedded lavas, in the central and southern portions of the study area; ii) layered pyroclastic fallout deposits, predominant in the northern and north-eastern portions of the study area (see also Karner et al., 2001, and Giordano et al., 2006, and references therein). The VT unit also includes subordinated sedimentary, fluvial and lacustrine deposits complexly interlayered with volcanites. These sediments, which represent a volumetrically minor portion of the VT unit (approximately 20%), prevail in the south-westernmost zone of the study area, close to the present day Tiber River valley. These sediments

record cyclic phases of valley incision and filling as river responses to glacio-eustatic sea level changes (Milli, 1997; Marra et al., 1998; Funicciello et al., 2008).

From the above, it is evident that the VT unit is the most heterogeneous unit in the Roman area in terms of spatial distribution of component lithotypes and related physical and mechanical parameters (see also the next paragraph).

3) Recent fluvial sediments (RA unit in Fig. 2; Late Pleistocene-Holocene) deposited by the Tiber and Aniene Rivers and their tributaries. This unit is composed of a basal lithosome of pebbles, sandy pebbles and gravels lying on an erosive lower boundary and passing upward to loose channel sands and poorly consolidated floodplain clays and silts, often rich in organic matter (Bozzano et al., 2000; Raspa et al., 2008). The alluvial deposits fill deep and narrow valleys that were previously carved into the Pleistocene units and even into the Plio-Pleistocene substratum by main rivers and their tributaries as a response to the Late Quaternary sea level fall and subsequent rise (Milli, 1997).

SUBSOIL DYNAMIC CHARACTERIZATION

A comprehensive characterization of the dynamic behavior of the Rome subsoil, due to the complexity of the geological units and of their geometry, is very difficult to assess. However, a brief description of physical and mechanical parameters of the main units and lithotypes is useful to explain the observed non-homogeneous distribution of shaking intensity due to site effects during the L'Aquila seismic events (see Tab. 2).

The over-consolidated clays and sands of the Plio-Pleistocene substratum (MMV unit) of the whole study area are characterized by a shear wave velocity $V_s=550-600$ m/s and a density $\rho=2.1$ g/cm³, at least for their uppermost portion (100-200 meters, Pagliaroli et al., 2011). These values were recently confirmed by an intense geophysical survey done in the Rome city centre at the Palatine Hill and surrounding archaeological areas (Fig. 2a). In this sector, the Plio-Pleistocene substratum was directly investigated for the uppermost twenty meters. Moreover, it was also possible to infer a V_s -depth profile throughout the MMV unit in the context of a 1D site-response analysis, by reproducing the terrain fundamental frequency as calculated by extensive seismic noise measurements (Pagliaroli et al., 2011). Measured and estimated V_s values within MMV are in good agreement with those by Rovelli et al. (1995) and Bozzano et al. (2008), but are definitely lower than the values presented by Fäh et al. (1995) and Donati et al. (1999) ($V_s=1000$ m/s and $1000 \leq V_s \leq 1500$ m/s, respectively) which, however, were not supported by borehole geophysical data.

Gravel, sands, and pelites of the PT unit display V_s values in the range of 650-700 m/s for gravel layers and 400 m/s for finer sediments. These values have been recently determined from geophysical tests carried out in the framework of the subway line C design (stored in the UrbiSIT database) and reported by Pagliaroli et al. (2011). Literature data generally provide a slightly lower mean value of V_s for this unit (400 m/s, by Fäh et al. 1995; and Rovelli et al. 1995).

The VT unit is characterized by a high degree of lithological heterogeneity, which is mirrored in the variability of physical and mechanical properties: V_s -measured values in the Palatine area range between 600 and 700 m/s for tuffs and cemented pyroclastites (VTa in Fig. 2), while interfingered sedimentary layers (VTc in Fig. 2) show lower V_s values, about 300-350 m/s (Pagliaroli et al., 2011).

Measures of dynamic parameter on the pyroclastic fallout deposits of the north and north-eastern portion of Rome (VTb in Fig. 2) are rare. The little available data (see Tab. 2) coming from the nearby northern boundary of the study area show V_s values for these deposits ranging between 300 and 400 m/s (CNR-IGAG, 2009).

In general, for the VT unit there is a good agreement of the presented values with those from literature (Rovelli et al., 1995; Donati et al., 1999; Bianchi Fasani et al., 2010), while a relevant discrepancy can be observed with Fäh et al. (1995), which propose $V_s=1.100$ m/s for volcanites.

Recent alluvial sediments (RA unit) show comparable V_s values for the main trunk and lateral tributaries, in the range of 250-300 m/s for the predominant sandy and clayey layers (Bozzano et al., 2008; Pagliaroli et al., 2011), while $V_s=650-700$ m/s can be attributed to the thin basal pebbly-gravel layer (Bozzano et al., 2008).

Finally, the anthropic backfill unit presents the highest variability of textural, compositional and physical-mechanical properties. V_s typically ranges from 150 to 300 m/s (Rovelli et al., 1995), while higher values (locally up to 800 m/s) are measured within archaeological areas where buried ruins can be found (Pagliaroli et al. 2011).

It is noteworthy that, due to the high lateral and vertical heterogeneity of lithotypes within each informal stratigraphic unit, the related dynamic parameters may show an equal spatial heterogeneity.

DATA AND METHODS

Macroseismic effects in the city of Rome, adverted during the mainshock and four strong aftershocks of the L'Aquila sequence (Tab. 1), were analyzed using data collected with the on-line macroseismic questionnaire of the Istituto Nazionale di Geofisica e Vulcanologia (INGV), which can be found at the web address <http://www.haisentitoilterremoto.it>. The web questionnaire, addressed to non-specialists, is mainly based on voluntary collaboration with ordinary people, but also on the contribution of a group of permanent compilers (about 11,000 people, distributed throughout the entire Italian territory) that are alerted by e-mail when an earthquake occurred near their municipality. The distribution of reports coming from Rome is shown in Figure 3.

Each questionnaire was treated with the method described in Sbarra et al., 2009 in order to extrapolate a probabilistic local estimate of the MCS intensity referred to the location of buildings (street addresses) as indicated by compilers. The intensity is assigned through the sum of the scores associated with the answers for every effect of the scale. If an effect is present in more than one macroseismic degree, the score is equally divided among all considered intensities. Assigning the probabilistic intensity to a questionnaire, we assume that the compiler and the observed building belong to the category of “many” of the MCS scale, the wider and thus the most probable category of people (Sbarra et al., 2009).

Local macroseismic intensity data were elaborated to obtain comparable values for all five events. Firstly we corrected the effect due to the observer floor position (Sbarra et al., 2011 submitted). In fact, analyzing 180,000 questionnaires coming from all over Italy in the last three years, we have found a correlation between intensity and observer floor position. For this reason, analyzed data were corrected in relation to the floor (Tab. 3). All data were then normalized by subtracting the global intensity of Rome for each event, varying from III MCS to IV-V MCS in the earthquakes analyzed (see MCS intensity in Tab. 1) and by compensating the attenuation effect with distance from the epicenter (Fig. 4). The attenuation law was experimentally derived using a total of 22,490 intensity values that referred

to towns and villages distributed all over central Italy for the five events analyzed in our web questionnaire (Fig.1). The data, normalized in respect to the global intensity of Rome of each earthquake, were then stacked together and fitted by a log-linear model in the form: $I - I_{Rome} = -1.2 \ln d + 5.3$, where d is the distance from the epicenter. In the present study a new relation has been fitted instead of using the general attenuation models calculated on classic survey intensity, because intensity data used here are assigned by a different method. The fundamental characteristics of the fitted attenuation laws have been retained, using the log-linear model of epicentral distance versus intensity. To test the influence of the attenuation model used, we tried to fit the relation using hypocentral distances: the differences in the city of Rome were negligible in the order of 0.01 MCS. Our experimental relation, in the distance range of 75-110 km pertaining to the city of Rome, is, however, inside the statistical uncertainty of the parameters of the attenuation law by Pasolini et al. (2008).

Intensity residual data of the five analyzed earthquakes (Fig. 5), obtained as shown, constitute the database used for the statistical analysis. In Tab. 1, the number of questionnaires from Rome collected for each event is shown, and about 50% of them refer to the mainshock. The variability of intensity data shown in Fig. 5 is intrinsic in the definition of MCS scale. A specific MCS intensity degree is represented by diverse seismic effects adverted in a single town. For example, the fourth MCS degree is characterized by 50% of people that feel the earthquake and by 50% of people that do not feel it. For this reason, it is important to consider the averaged values of a sufficient number of MCS intensity residuals. Data were then filtered and interpolated in order to obtain a continuous residual smoothed map, just to have a graphical support to compare with geological maps (Fig 5). An interpolation method was used to obtain a grid with a step of 400 m, averaging data inside a radius of 2.5 km weighted with the inverse of distance (the same parameters were used for geological maps interpolation of Figs. 2c, 2d). Grid nodes were interpolated if the local point density was greater or equal to three intensity data per km². Areas with a lower density of data correspond to non-urbanized zones.

The acoustic effect is another aspect associated to the earthquake. In the web-based macroseismic questionnaire, there is a specific question on the perception of the earthquake sound. Data, consisting of 1 'heard' and 0 'not heard' options, were interpolated and filtered (Tosi et al., 2000) with the same procedure used for intensity residuals producing the map shown in Fig. 6. Earthquake sounds have been mostly explained as acoustic waves generated by the compressive waves that travel in the earth (Hill et al., 1976). For this reason, its perception is influenced by the P wave velocity of the near-surface layer. We use the sound data as a completely independent source of information because it is not used for evaluation of macroseismic intensity.

RESULTS AND DISCUSSION

Amplification effects are mainly due to lithology, subsoil geometries and topography, all of these factors having a complex interaction. The intensity residual data were compared and interpreted in the light of geological reconstructions (Figs. 2c, 2d) on the scale of the whole city. To reveal the presence of amplification and de-amplification areas in the urban territory of Rome, with the latter included inside the ring (GRA) highway, we calculated the mean values and standard deviations of residual data inside the specific areas of geological interest shown in Fig. 7.

In the NE zone of the city, there is the presence of the Paleotiber Graben (Fig. 2a), filled up by deposits of the Paleotiber unit (PT unit in Fig. 2b). It is well known that buried valleys can induce seismic amplification, as shown by Pergalani et al. (2006). In alluvial valleys, or in basins with geometrical features similar to the Paleotiber Graben (W/T

ratio = 26.6, with W , width = 4 km; T , thickness = 150 m), as in the case of the Nizza Basin, the maximum amplification is expected in the middle of the valley (Semblat et al., 2000). Moreover, Raptakis et al. (2000) observed that the amplification of ground motion inside a graben is due not only to the resonance of vertically propagated shear waves but also to locally generated surface waves, and it may be higher in the centre of the structure. Combining the geometry effect (shape ratio) with the soil layering effect due to the impedance contrast between different interbedded soil layers (Bard and Riepl-Thomas, 1999), there could be an increase of amplification of seismic motion and a duration lengthening in the central part of the basin (Semblat et al., 2005). In order to verify the presence of an amplification area in the central portion of the graben and to test its significance, we calculated the mean value of residuals inside boundary 1 in Fig. 7, traced at 1 km of distance from the graben axis, it resulted to be 0.19. This value has been compared to the average of residuals of the whole city (-0.05, Tab. 4), excluding points inside the central area of the Paleotiber Graben and inside the Tiber alluvial sediments (inside boundaries 1 and 2 of Fig. 7). The T statistical test shows that, even if the average value of boundary 1 is quite small, it is significantly different (at 1⁰/₀₀) from the whole city average. The same test was separately performed for the five earthquakes, giving the same results of the combined analysis, with a significance at worst of 2 %.

Due to the difficulty in knowing the real geometry of the multilayer structure inside the Paleotiber Graben, it is difficult to explain the cause of local amplification evidenced by the macroseismic data (Fig. 5). By the way, the impedance contrast occurring at the various lithological boundaries within the multilayer filling of the graben could have determined wave channelling within the less rigid, thick pelitic intervals, and consequent amplification effects (Fig. 8).

About morphological and geological effect on amplification, it is worth noting that the Aniene River, with the related soft-sediment bearing floodplain, is imposed on the Paleotiber Graben (Fig. 2b). Amplification of macroseismic intensity on the Aniene sediments was indeed observed by Tertulliani et al. (1996) in the analysis of the Rome earthquake of 12 June 1995, and by Cifelli et al. (2000) and Donati et al. (2008) for the two Umbria-Marche earthquakes of September 1997. On the other hand, residuals from the present study (Fig. 5) show higher values not only on the Aniene River plain but also on surrounding areas. The mean value of residuals inside the Aniene alluvial sediments is lower than the average calculated in the central area of the Paleotiber Graben (Tab. 4, Fig. 7). Thus, in this case, the deep geology seems to be the main amplification factor.

The Tiber sediments should also represent an amplification zone in accordance with previous works (Ambrosini et al., 1986; Molin and Guidoboni, 1989; Tertulliani et al., 1996; Cifelli et al., 2000; Donati et al., 2008). The average of the residuals inside boundary 2 is positive (0.15), although smaller than that relative to the graben axis. The T test, performed on the averages calculated inside the Tiber alluvial sediments (boundary 2) and the entire city excluding points in boundaries 1 and 2 (Fig. 7), indicates a significant difference at 3⁰/₀₀ (Tab. 4).

In order to have a further validation of the statistical significance of intensity residual averages, we randomly took three groups of 450, 532 and 2,713 points (respectively the number of points inside Tiber alluvial sediments, the central area of the Paleotiber Graben, and other remaining areas of Rome, see Fig. 7 and Tab. 4), 100,000 times, and we calculated the average of each group. The frequency histograms of the 100,000 averages (Fig. 9) show that the real values 0.19 and 0.15 in the cases respectively of Fig. 9a and Fig. 9b are very unlikely in a random selection. Instead the real value for the entire city (-0.05) is, like the random ones, very near to zero (Fig. 9c).

The two amplification zones located on the Tiber valley and on the Paleotiber Graben are evident in Fig. 10, where the profile of the interpolated grid of residuals (Fig. 5) is compared to geological section AA' (Fig. 2b) to show the entity of amplification due to depth with respect to near-surface geology.

Our experimental results show that the Paleotiber sediments can cause an amplification of seismic waves. This result is supported by the simulation of Fäh et al. (1995), but it was not confirmed by a previous macroseismic analysis (Cifelli et al., 2000).

In the numerical simulation by Fäh et al. (1995), the averages of amplification factors of acceleration from the Paleotiber Graben and the Tiber valley, with respect to the bedrock, varies between 1 and 2. We decided to take into consideration the averages instead of the maximum amplification factors, because we compared these values with those calculated on averaged intensities. Considering the interpolated intensities for the main shock of 6 April, made with the same method used for total data, a maximum value on the Paleotiber Graben of 4.9 and on the Tiber valley of 4.6 MCS can be observed, whereas the area without amplification (i.e. the zone along the profile AA' of Fig. 2a between the Tiber valley and the Paleotiber Graben) has a value of 4 MCS. By using the empirical relation $\log pga = 0.52 + 0.22I$ of Margottini et al. (1992) where I is the MCS intensity, the corresponding amplification factors were calculated: 1.6 for the Paleotiber Graben and 1.4 for the Tiber valley, comparable with those coming from numerical simulation (Fäh et al., 1995).

In the seismic microzonation by Fäh et al. (1995), the maximum amplification is expected along the edges of the Paleotiber Graben instead of in the center. This difference with respect to the present study could be due to i) the physical and mechanical parameters used by the cited authors in their simulation (see previous subsoil dynamic characterization), and ii) the geological model used by authors. In particular, Fäh et al. (1995) showed a thickness of volcanites greater at the center (60 m) and thinner at the edges of the Paleotiber Graben, whereas the correlation of available boreholes allowed us to reconstruct a VT unit with almost constant thickness (approximately 20 m in Fig. 2d).

Looking the Tiber plain at a detailed scale, we can observe that the amplification is not uniform, and some zones without amplification are present. We compared the intensity residual map of this area (Fig. 11a) with the interferometric deformation velocity map (Manunta et al., 2008; Fig. 11b). This map was elaborated with the differential synthetic aperture radar interferometry technique, exploiting SAR images at full spatial resolution (of the order of 5-20 m). Manunta et al. (2008) showed that the major contribution to the detected displacement is due to the differential consolidation of alluvial sediments. The sectors of the Tiber alluvial plain where seismic amplification is higher coincide with the more subsiding zones (points in yellow, orange and red colors, Fig 11b), which are characterized by poorly consolidated floodplain deposits. On the contrary, the areas of the alluvial plain with low macroseismic intensity residuals correspond to steady zones such as the historical centre (bold line in Fig. 11). Here indeed, consolidation processes ceased because sediments have been subjected for a long time (up to 2.5 ka) by imposed external loads such as buildings, deposition of a 10-20 m thick anthropic backfill, dewatering and water pumping. The difference of amplification in the Tiber alluvial sediments is confirmed by the statistical T test performed on the averages calculated using residual intensity points included in boundary 2 (Fig. 7), respectively inside (-0.04) and outside (0.17) the historical centre (boundary 4, Fig. 7). The test indicates a significant difference with a probability of 2.5%.

A further wide zone of amplification effects is located in the south-westernmost portion of the study area, just outside the GRA highway and close to the Acilia area (Figs. 2a and 5). It is difficult in this case to find a direct explanation. For this reason, we will analyze this topic in more detail in a future study.

Interesting relationships appear when comparing geological reconstructions with the distribution of acoustic effect perception (Fig. 6). Data on earthquake sound derived from questionnaires referred only to the main shock, but are independent from intensity residuals because they are not used in the evaluation of macroseismic intensity. It can be noted that few people along the Tiber valley heard the acoustic effect, while in other areas a greater number of questionnaires reported the occurrence of this rumble. To check the significance of this difference, the Chi squared test was performed on the frequencies of 0 (not heard) and 1 (heard) inside the Tiber valley (boundary 2 Fig. 7) and in all of the other areas: the distributions resulted different at 2% of significance. The explanation of this behavior is in the correlation between the perception of the acoustic effect and the seismic wave velocity of the outcropping layer: higher in the substratum than in alluvial sediments.

CONCLUSIONS

The illustrated method allowed the investigation of amplification areas using low macroseismic intensities, increasing the number of collected data coming even from recently urbanized areas. The comparison of macroseismic data from on-line questionnaires with detailed geological reconstructions provides evidence of some amplification areas unknown by historical macroseismic observation in Rome, in particular the Paleotiber Graben. Thus it is shown how the contribution of the deep geology must be considered, and how it is as important as the surface geology in microzonation studies. Due to the difficulty in making a reliable seismic propagation model reflecting the complex geology in sufficient detail, we propose using macroseismic intensity residuals as a contribution to the elaboration of hazard maps. But we want to stress the possibility of non-linear behavior in case of higher shaking in respect to the low intensities analyzed in this paper. Finally, some aspects never investigated before were evidenced, such as the correlation between seismic amplification in recent alluvial settings and subsiding zones, and between seismic sound perception and near-surface geology.

ACKNOWLEDGEMENTS

Geological setting derives from the UrbiSIT Project (<http://www.urbisit.it> project manager: Dr. Gian Paolo Cavinato) funded for CNR-IGAG by the DPC (Italian Civil Protection National Service). Macroseismic analysis was supported by the DPC S1 and S3 Projects. The authors thank R. Lanari and M. Manunta (CNR-IREA) for Figure 11b, G.P. Cavinato for useful discussions on the geological model, S. Barba and A. Rovelli for helpful advice and A. Pagliaroli (CNR-IGAG) for his important contribution on the physical and mechanical characterization of the geological units. E. Di Luzio contributed to the geological model of the city of Rome when he was employed by CNR-IGAG. D. Sorrentino is acknowledged for the system administration of the entire ICT architecture of <http://www.haisentitoilterremoto.it> (the INGV macroseismic web site) and for software development.

REFERENCES

- Ambrosini S, Castenetto S, Cevolan F, Di Loreto, E, Funicello, R, Liperi, L, and Molin, D (1986) Risposta sismica dell'area urbana di Roma in occasione del terremoto del Fucino del 13-1-1915. *Mem. Soc. Geol. It.* 35: 445–452.
- Bakir BS, Ozkan MY, and Ciliz S (2002) Effects of basin edge on the distribution of damage in 1995 Dinar, Turkey earthquake. *Soil Dyn Earth Eng* 22: 335–345. doi:10.1016/S0267-7261(02)00015-5
- Bard PY, and Riepl-Thomas J (1999) Wave propagation in complex geological structures and their effects on strong ground motion in: *Wave motion in Earthquake Engineering*, edited by Kausel and Manolis WIT Press, 37-95.
- Bianchi Fasani G, Bozzano F, Cercato M (2011) The underground cavity network of south-eastern Rome city (Italy): an evolutionary geological model oriented to hazard assessment, *Bull. Eng. Geol. Environ.* doi: 10.1007/s10064-011-0360-0.
- Bozzano F, Andreucci A, Gaeta M, Salucci R (2000) A geological model of the buried Tiber River valley beneath the historical centre of Rome. *Bull. Eng. Geol. Env.* 59:1–21. doi:10.1007/s100640000051.
- Bozzano F, Caserta A, Govoni A, Marra F, Martino S (2008) Static and dynamic characterization of alluvial

deposits in the Tiber River Valley: New data for assessing potential ground motion in the City of Rome. *Journal of Geophysical Research* 113:1-21. doi: 10.1029/2006JB004873.

Carlino S, Cubellis E, Marturano A (2009) The catastrophic 1883 earthquake at the island of Ischia (southern Italy): macroseismic data and the role of geological conditions. *Nat. Hazards* 52, 231–247. doi: 10.1007/s11069-009-9367-2.

Cifelli F, Donati S, Funicello F, Tertulliani A (2000) High-Density Macroseismic Survey in Urban Areas. Part 2: Results for the City of Rome, Italy. *Bull. Seism. Soc. Am.* 90:298–311. doi:10.1785/0119990097.

CNR-IGAG (2009). Relazione geologico-tecnica e sismica sull'Area della Ricerca di Roma-RM1 Montelibretti. Internal CNR report, Montelibretti (Rome), 9 pp. and addenda.

Dengler LA, Dewey JW (1998) An Intensity Survey of Households Affected by the Northridge, California, Earthquake of 17 January 1994, *Bull. Seism. Soc. Am.* 88:441-462.

Donati S, Cifelli F, F Funicello (2008) Indagini macrosismiche ad alta densità per lo studio del risentimento sismico nella città di Roma, in: *La Geologia di Roma - dal centro storico alla periferia*. Mem. Descr. Carta Geol. D'It., vol 80, edited by R. Funicello et al., pp. 13-30, S.EL.CA., Firenze.

Donati S, Funicello R, Rovelli A (1999) Seismic response in archaeological areas: the case-histories of Rome. *Jour. App. Geoph.* 41:229-239.

Fäh D, Iodice C, Suhadolc P, Panza GF (1995) Application of numerical simulations for a tentative seismic microzonation of the city of Rome. *Annali di Geofisica* 38:607-615.

Florindo F, Karner DB, Marra F, Renne PR, Roberts AP, Weaver R (2007) Radioisotopic age constraints for Glacial Terminations IX and VII from aggradational sections of the Tiber River delta in Rome, Italy. *Earth and Planetary Science Letters*. 256:61-80, doi:10.1016/j.epsl.2007.01.014.

Funicello R, Praturlon A, Giordano G (2008) *La Geologia di Roma - dal centro storico alla periferia*. Mem. Descr.

Carta Geol. D'It. vol. 80, 765, S.EL.CA., Firenze.

Giammarinaro MS, Tertulliani A, Galli G, Leta M (2005) Investigation of Surface Geology and Intensity Variability in the Palermo, Italy, Urban Area after the 6 September 2002 Earthquake. *Bull. Seism. Soc. Am.* 95:2318-2327, doi:10.1785/0120040214.

Giordano G, De Benedetti AA, Diana A, Diano G., Gaudio F, Marasco F, Miceli M, Mollo S, Cas RAF, Funicello R (2006) The Colli Albani mafic caldera (Roma, Italy): Stratigraphy, structure and petrology. *Journal of Volcanology and Geothermal Research.* 155:49-80, doi:10.1016/j.jvolgeores.2006.02.009.

Hill DP, Fisher FG, Lahr KM, Coakley JM (1976) Earthquake sounds generated by body- wave ground motion. *Bull. Seismol. Soc. Am.* 66:1159-1172.

Karner DB, Marra F, Renne PR (2001) The history of the Monti Sabatini and Alban Hills volcanoes: groundwork for assessing volcanic-tectonic hazards for Rome. *Journal of Volcanology and Geothermal Research.* 107:185-219.

Kayano I (1990) Distribution of various effects and damages caused by earthquakes and of seismic intensities on the basis of questionnaire surveys: a newly developed group survey method. *Bull. Earthq. Res. Inst., Univ. Tokyo* 65:463–519.

Lee SJ, Komatitsch D, Huang BS, Tromp J (2009) Effects of Topography on Seismic-Wave Propagation: An Example from Northern Taiwan. *Bull. Seism. Soc. Am.* 99:314–325. doi:10.1785/0120080020.

Manunta M, Marsella M, Zeni G, Sciotti M, Atzori S, Lanari R (2008) Two-scale surface deformation analysis via the SBAS-DInSAR technique: A case study of the city of Rome, Italy. *International Journal of Remote Sensing* 29:1665-1684. doi: 10.1080/01431160701395278.

Margottini C, Molin D, Serva L (1992) Intensity versus ground motion: a new approach using Italian data, *Eng. Geol.* 33:45–58.

Marra F, Rosa C, De Rita D, Funicello R (1998) Stratigraphic and tectonic features of the middle pleistocene

sedimentary and volcanic deposits in the area of Rome (Italy). *Quaternary International* 47-48:51–63.
doi:10.1016/S1040-6182(97)00070-0.

Milli S (1997) Depositional settings and high-frequency sequence stratigraphy of the middle-upper pleistocene to Holocene deposits of the Roman basin, *Geologica Romana* 33:99–136.

Molin D, Guidoboni E (1989) Effetto fonti, effetto monumenti a Roma: i terremoti dall'antichità ad oggi, in: I terremoti prima del Mille in Italia e nell'Area Mediterranea. edited by E. Guidoboni (Eds.), pp. 194–223, ING, Bologna.

Ocola L (2008) Procedure to estimate maximum ground acceleration from macroseismic intensity rating: application to the Lima, Perú data from the October-3-1974-8.1-Mw earthquake. *Advances in Geosciences* 14:93-98. doi:10.5194/adgeo-14-93-2008.

Pagliaroli A, Quadrio B, Sanò T, Sabetta F, Castenetto S, Naso G, Moscatelli M, Lanzo G, Di Fiore V (in press) Risposta sismica locale dell'area archeologica comprendente il Colle Palatino, i Fori e il Colosseo, in R. Cecchi (Ed.) "Roma archaeologia. Interventi per la tutela e la fruizione del patrimonio archeologico; terzo rapporto", Mondadori Electa S.p.A., Milano.

Panou AA, Theodulidis N, Hatzidimitriou P, Stylianidis K, Papazachos CB (2005) Ambient noise horizontal-to-vertical spectral ratio for assessing site effects estimation and correlation with seismic damage distribution in urban environment: the case of city of Thessaloniki (Northern Greece). *Soil Dyn. Earthqu. Eng.* 25:261–274.
doi:10.1016/j.soildyn.2005.02.004.

Pasolini C, Gasperini P, Albarello D, Lolli B, D'Amico C (2008) The Attenuation of Seismic Intensity in Italy, Part I: Theoretical and Empirical Backgrounds. *Bull. Seism. Soc. Am.* 98:682 - 691.

Pergalani F, De Franco R, Compagnoni M, Caielli G (2006) Evaluation of site effects using numerical and experimental analyses in Citta' di Castello (Italy). *Soil Dyn. Earthqu. Eng.* 26:941-951.
doi:10.1016/j.soildyn.2006.02.003.

Raptakis D, Chavez-Garcia FJ, Makra K, Pitilakis K (2000) Site effects at Euroseistest-I. Determination of the valley structure and confrontation of observations with 1D analysis. *Soil Dyn. Earthqu. Eng.* 19:1-22. doi:10.1016/S0267-7261(99)00025-1.

Raspa G, Moscatelli M, Stigliano F, Patera A, Folle D, Vallone R, Mancini M, Cavinato GP, Milli S, Costa JFCL (2008) Geotechnical characterization of the upper Pleistocene-Holocene alluvial deposits of Roma (Italy) by means of multivariate geostatistics: crossvalidation results, *Engineering Geology* 101: 251-268. doi:10.1016/j.enggeo.2008.06.007.

Rovelli A, Malagnini L, Caserta A, Marra F (1995) Using 1-D and 2-D modelling of ground motion for seismic zonation criteria: results for the city of Rome. *Annali di Geofisica* 38:591-605.

Sbarra P, Tosi P, De Rubeis V (2009) Web based macroseismic survey in Italy: method validation and results, *Nat. Hazard* 54:563-581. doi: 10.1007/s11069-009-9488-7.

Sbarra P, Tosi P, De Rubeis V, Rovelli, A, (2012) Influence of observation floor and building height on macroseismic intensity, *Seismological Research Letters* (in print).

Seekins L C, Boatwright J (1994) Ground motion amplification, geology, and damage from the 1989 Loma Prieta earthquake in the City of San Francisco. *Bull. Seism. Soc. Am.* 84:16-30.

Semblat J F, Duval AM, Dangla P (2000) Numerical analysis of seismic wave amplification in Nice (France) and comparisons with experiments. *Soil Dynamics and Earthquake Engineering* 19:347-362. doi:10.1016/S0267-7261(00)00016-6.

Semblat J F, Dangla P, Kham M, Duval AM (2002) Seismic site effects for shallow and deep alluvial basins: in-depth motion and focusing effect, *Soil Dynamics and Earthquake Engineering* 22:849-854. doi:10.1016/S0267-7261(02)00107-0.

Semblat JF, Kham M, Parara E, Bard PY, Pitilakis K, Makra K, Raptakis D (2005) Seismic wave amplification: basin geometry vs soil layering, *Soil Dynamics and Earthquake Engineering* 25:529-538. DOI :

10.1016/j.soildyn.2004.11.003.

Sieberg A (1930) Scala MCS (Mercalli-Cancani-Sieberg). *Geologie der Erdbeben, Handbuch der Geophysik* 2:552-555.

Signorini R (1939) Risultati geologici della perforazione eseguita dall'AGIP alla mostra autarchica del minerale nel Circo Massimo di Roma. *Bollettino della Società Geologica Italiana*, 58:60-63.

Sousa ML, Oliveira CS (1997) Hazard Mapping Based on Macroseismic Data Considering the Influence of Geological Conditions. *Nat. Hazards* 14:207-225. doi:10.1007/BF00128267.

Tertulliani A, Tosi P, De Rubeis V (1996) Local seismicity in Rome (Italy): recent results from macroseismic evidences, *Annali di Geofisica* 39:1235–1240.

Toshinawa T, Taber JJ, Berill JB (1997) Distribution of ground-motion intensity inferred from questionnaire survey, earthquake recordings, and microtremor measurements - a case study in Christchurch, New Zealand, during the 1994 Arthurs Pass Earthquake. *Bull. Seism. Soc. Am.* 87:356-369.

Tosi P, De Rubeis V, Tertulliani A, Gasparini C (2000) Spatial patterns of earthquake sounds and seismic source geometry. *Geophys. Res. Lett.* 27:2749–2752. doi:10.1029/2000GL011377.

Table 1. Basic parameters of L'Aquila sequence main earthquakes.

Date and time (UTC)	Coordinates	MI	Depth (km)	Number of questionnaires	MCS intensity
6 April 2009 01:32	42° 20' 2"N 13° 20' 2"E	5.8	8.8	1929	4.45
7 April 2009 17:48	42° 16' 30"N 13° 27' 50"E	5.3	15.1	527	3.71
9 April 2009 00:53	42° 29' 2"N 13° 20' 35"E	5.1	15.4	301	3.43
9 April 2009 19:38	42° 30' 4"N 13° 21' 22"E	4.9	17.2	477	3.32
13 April 2009 21:14	42° 30' 14"N 13° 21' 47"E	4.9	7.5	461	3.23

Table 2. Range of density and shear wave velocity for the main geological units described in the text (see also Fig. 2).

Unit	ρ (g/cm ³)	Vs (m/s)	References
Anthropic backfill (AB)	1.7-1.9	150-300	Rovelli et al., 1995; Pagliaroli et al. 2011
Recent fluvial deposits (RA)	1.8-1.9	250-300 (sands and pelites) 650-700 (gravels)	Bozzano et al., 2008; Pagliaroli et al., 2011
Volcanic unit (VT)	1.7-1.9	600-700 (lithified pyroclastic flow deposits:VTa) 300-400 (un-lithified pyroclastic fallout deposits:VTb) 300-350 (sedimentary interbedded layers:VTc)	Rovelli et al., 1995; Donati et al., 1999 ; CNR-IGAG, 2009; Bianchi Fasani et al., 2010; Pagliaroli et al., 2011
Paleotiber unit (PT)	2-2.2	400 (sands and pelites) 650-700 (gravels)	Fäh et al., 1995; Rovelli et al. 1995; Pagliaroli et al., 2011
Geologic bedrock	2.1	550-600	Rovelli et al. 1995; Bozzano et al., 2008;

(MMV)			Pagliaroli et al., 2011
-------	--	--	-------------------------

Table 3. Floor correction factors.

Floor number	Floor correction factors
-1 0	0.10
1 2	-0.05
3 4	-0.13
5 6	-0.18
≥ 7	-0.27

Table 4. Comparison of mean intensity residuals in Rome sub-areas.

Area	Mean intensity residual (MCS)	Number of questionnaires	Standard deviation
Tiber alluvial sediments (boundary 2, Fig. 7)	0.15	450	0.87
Central area of Paleotiber Graben (boundary 1, Fig. 7)	0.19	532	0.89
Other (entire city excluding boundaries 1 and 2, Fig. 7)	-0.05	2713	0.87
Aniene alluvial sediments (Fig. 7)	0.11	322	0.92
Tiber alluvial sediments (boundary 2, Fig. 7) inside historical centre (boundary 3)	-0.04	57	0.87
Tiber alluvial sediments (boundary	0.17	393	0.87

2, Fig. 7) outside historical centre (boundary 3)			
--	--	--	--

FIGURE CAPTIONS

Figure 1

Filtered macroseismic intensity fields of five main earthquakes which occurred during L'Aquila sequence.

Figure 2

(a) Simplified geological map of Rome, indicating the geological structures and the track of the geological section A-A'; note that only the anthropic backfill with thickness ≥ 15 meters is mapped. (b) Geological section A-A'; (c) Thickness map of the PT stratigraphic unit; no erosion after the last glacio-eustatic oscillation is considered. (d) Thickness map of the VT stratigraphic unit; no erosion after the last glacio-eustatic oscillation is considered.

Figure 3

Distribution of macroseismic questionnaires in the urban area of Rome.

Figure 4

Macroseismic intensity attenuation versus epicentral distance of all five analyzed earthquakes. Intensities are town-averaged and normalized as deviations from Rome intensity value.

Figure 5

Macroseismic intensity residuals map of Rome produced by the five main earthquakes of the L'Aquila sequence (Tab. 1). Residual intensity data are shown. The amplification areas are represented in orange-red colours, and the de-amplification areas are represented in green.

Figure 6

6 April 2009 earthquake sound perception distribution interpolated map and original points.

Figure 7

Boundaries of areas used to calculate averages of intensity residual for the statistical tests. The colors used to fill the boundaries refer to the residual average values and are the same used for intensity residuals of Fig. 5.

Figure 8

Conceptual scheme showing the stratigraphic relations between the deposits filling and covering the Paleotiber Graben. Shear wave velocity is reported for every unit (see Tab. 2). The ideal track of the sketch is marked on Fig. 2a. See text for further details.

Figure 9

Histograms of the averages calculated on 450 (a), 532 (b) and 2713 (c) residuals randomly chosen, 100,000 times, among all data points. The number of points are respectively equal to Tiber alluvial sediments sample, central area of Paleotiber Graben sample and remaining area of Rome sample. See Fig. 7 and Tab. 3.

Figure 10

Comparison between the profile of the interpolate grid of residuals (Fig. 5) and geological section AA' (Fig. 2b). AB=anthropic backfill; RA=alluvial deposits; VT=volcanic deposits; PT=Paleotiber deposits; MMV=plio-pleistocene bedrock.

Figure 11

(a) Macroseismic intensity residuals map (enlarged portion of Fig. 5); (b) subsiding and stable zones as evidenced by interferometric velocity maps (modified after Manunta et al., 2008).

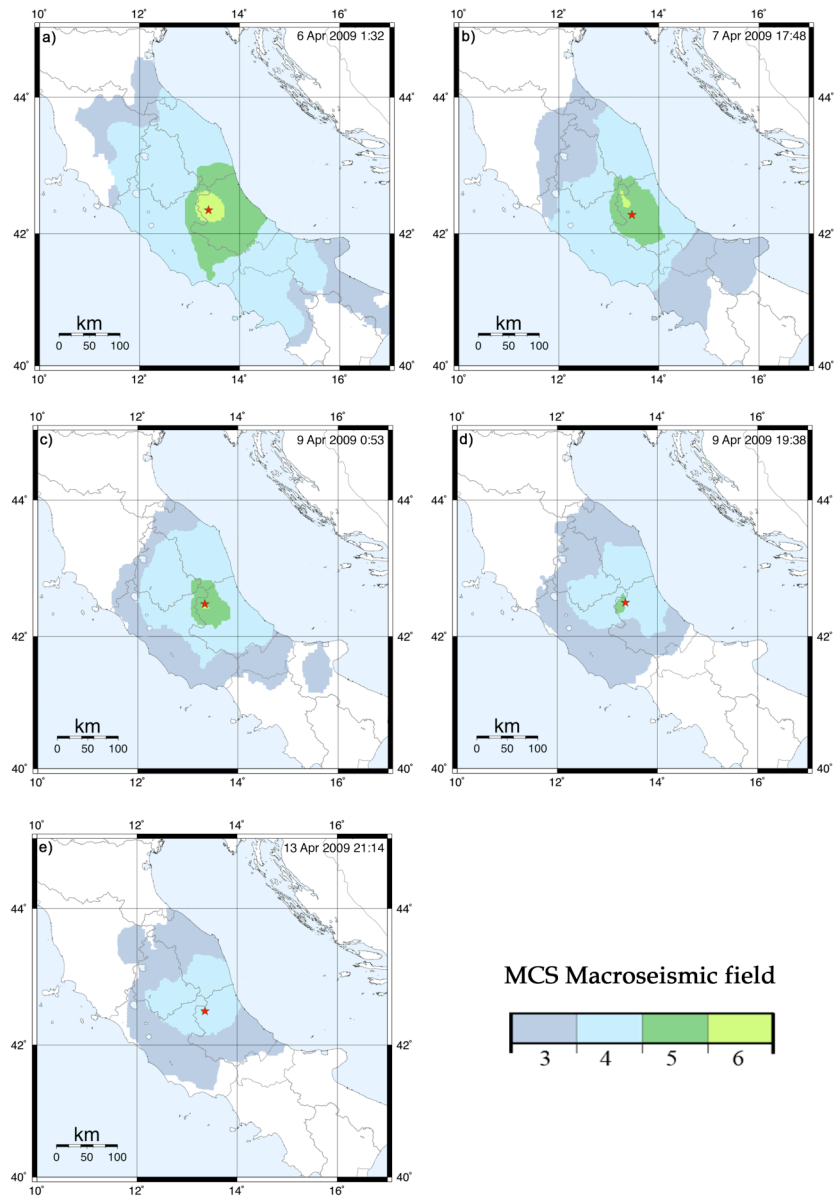


Figure 1

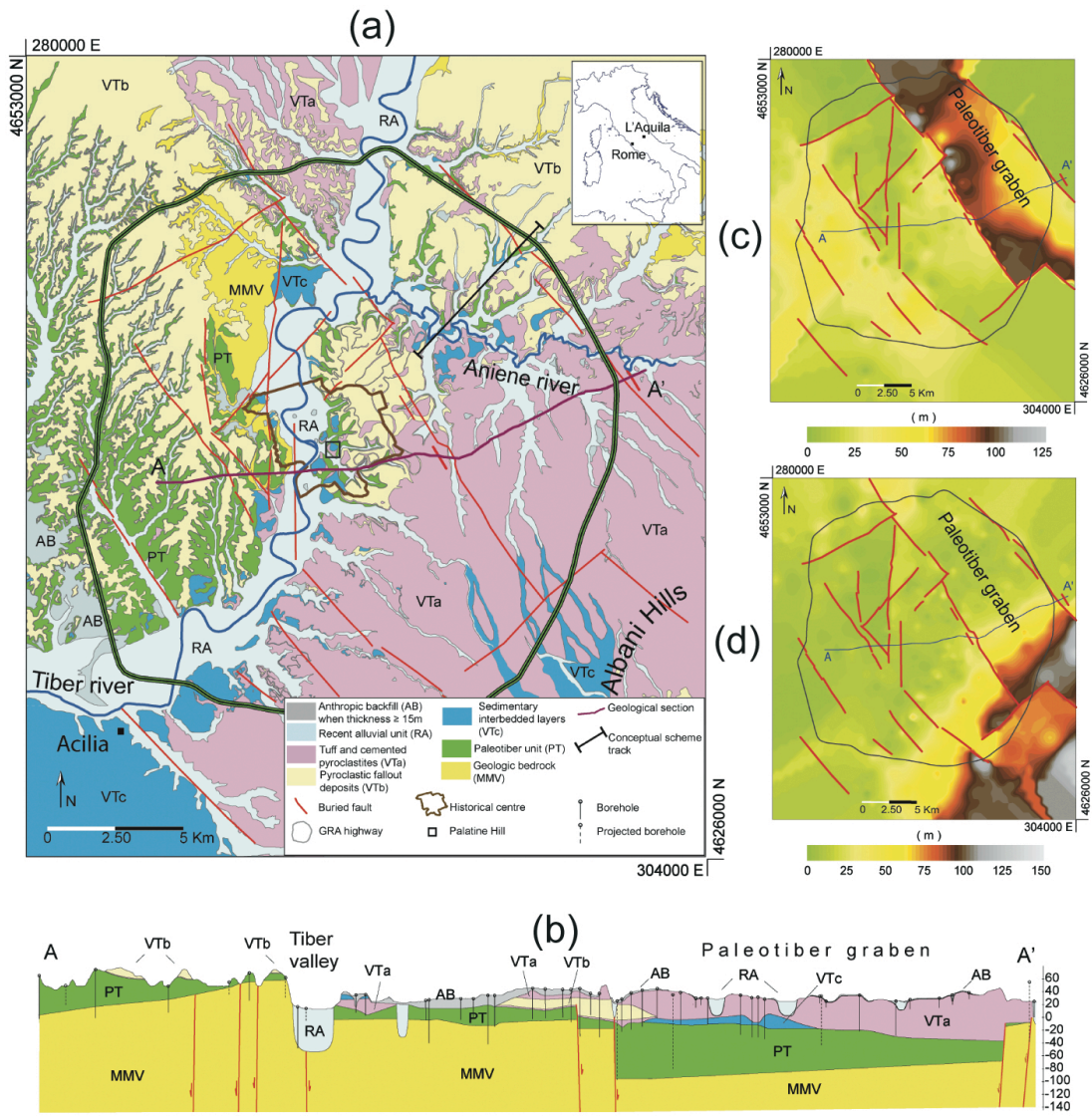


Figure 2

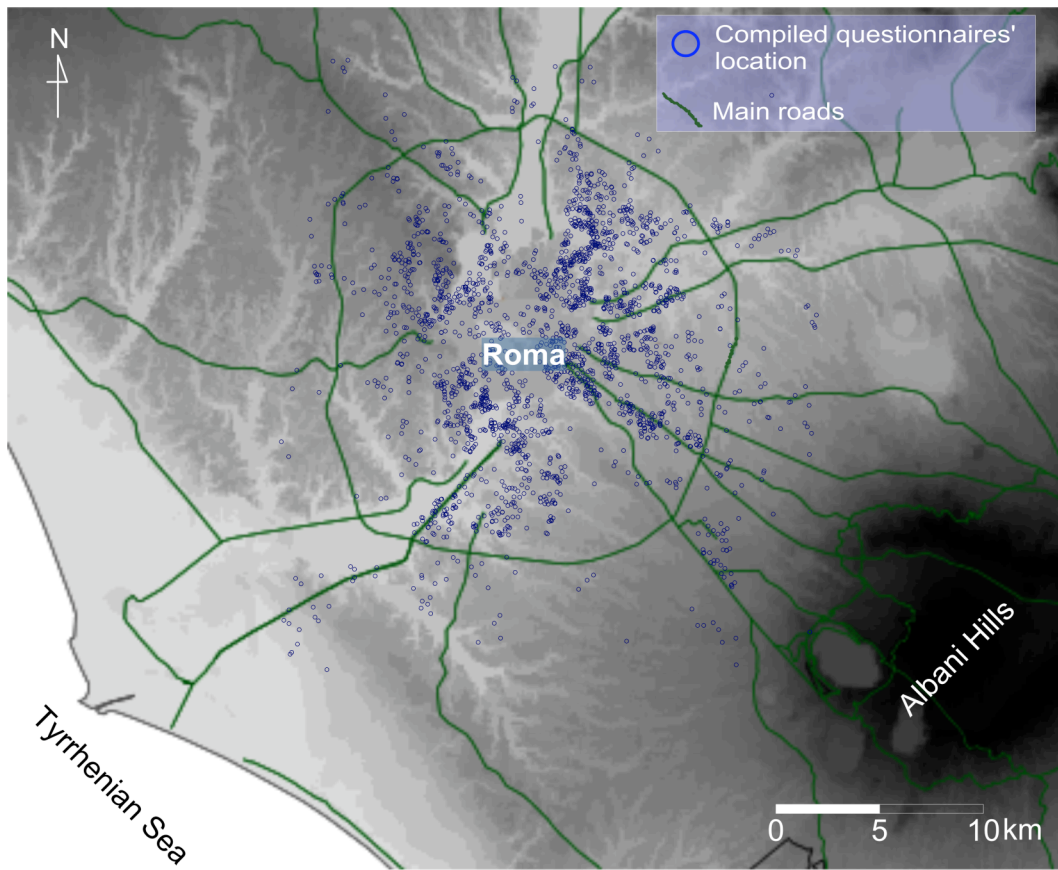


Figure 3

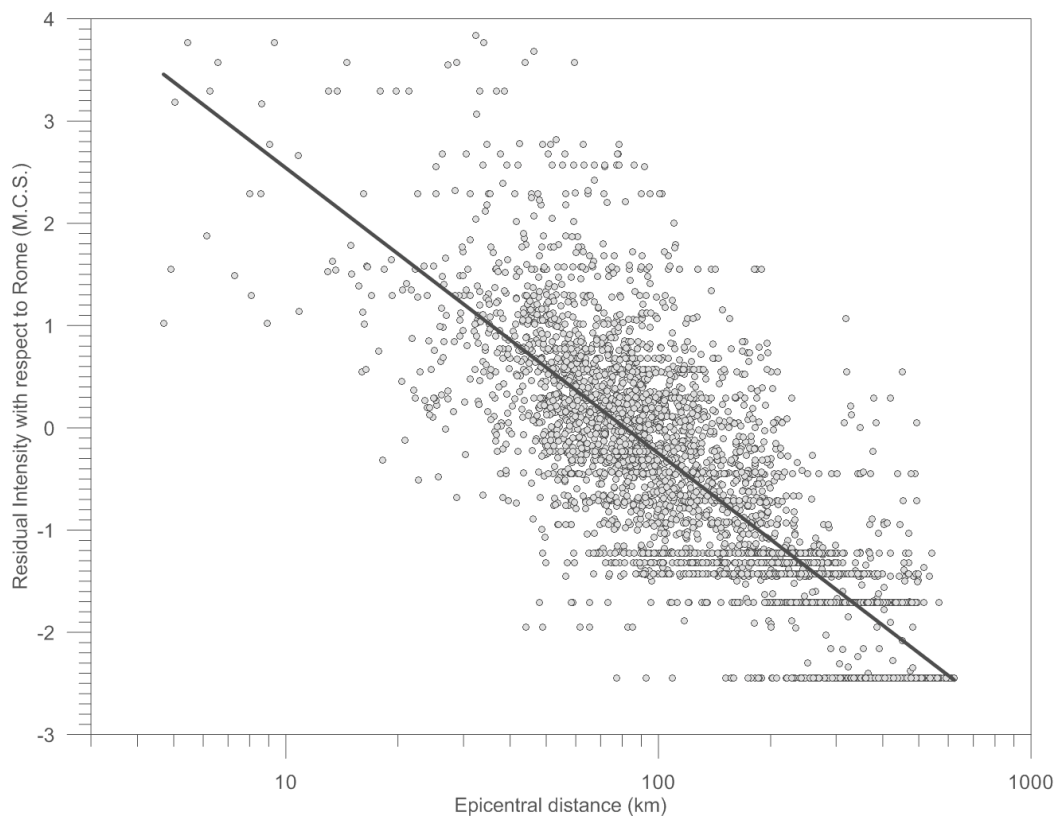


Figure 4

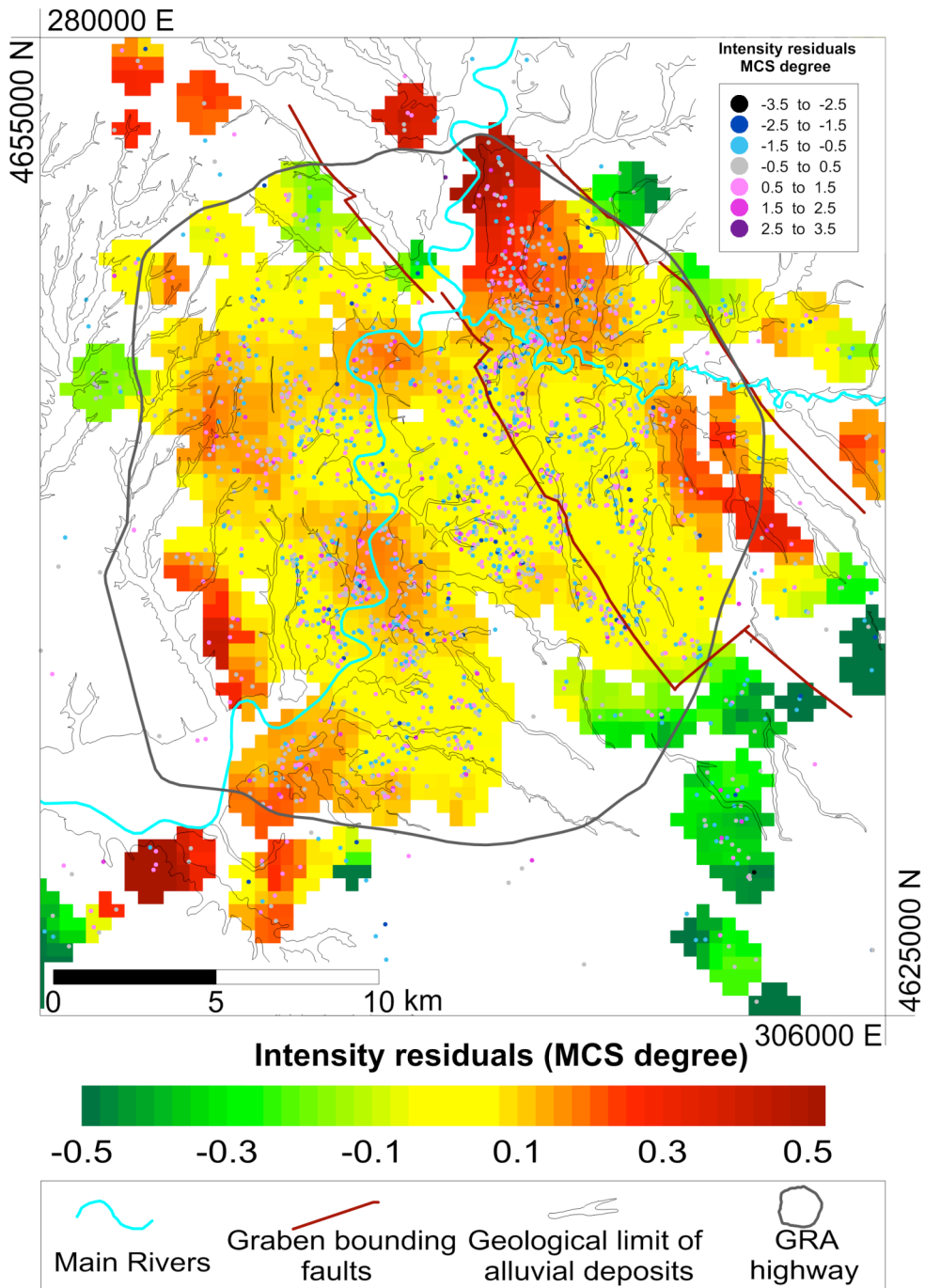


Figure 5

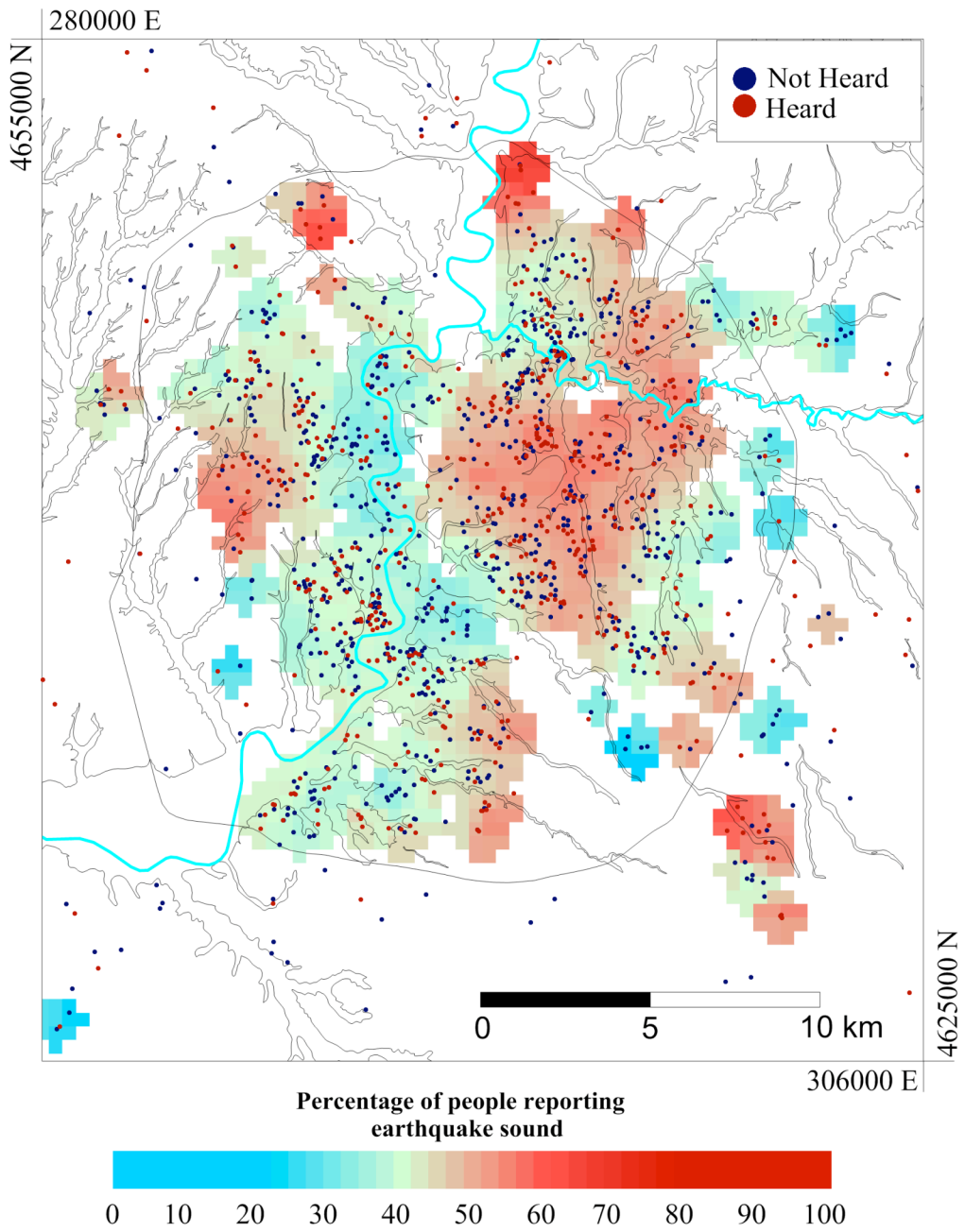


Figure 6

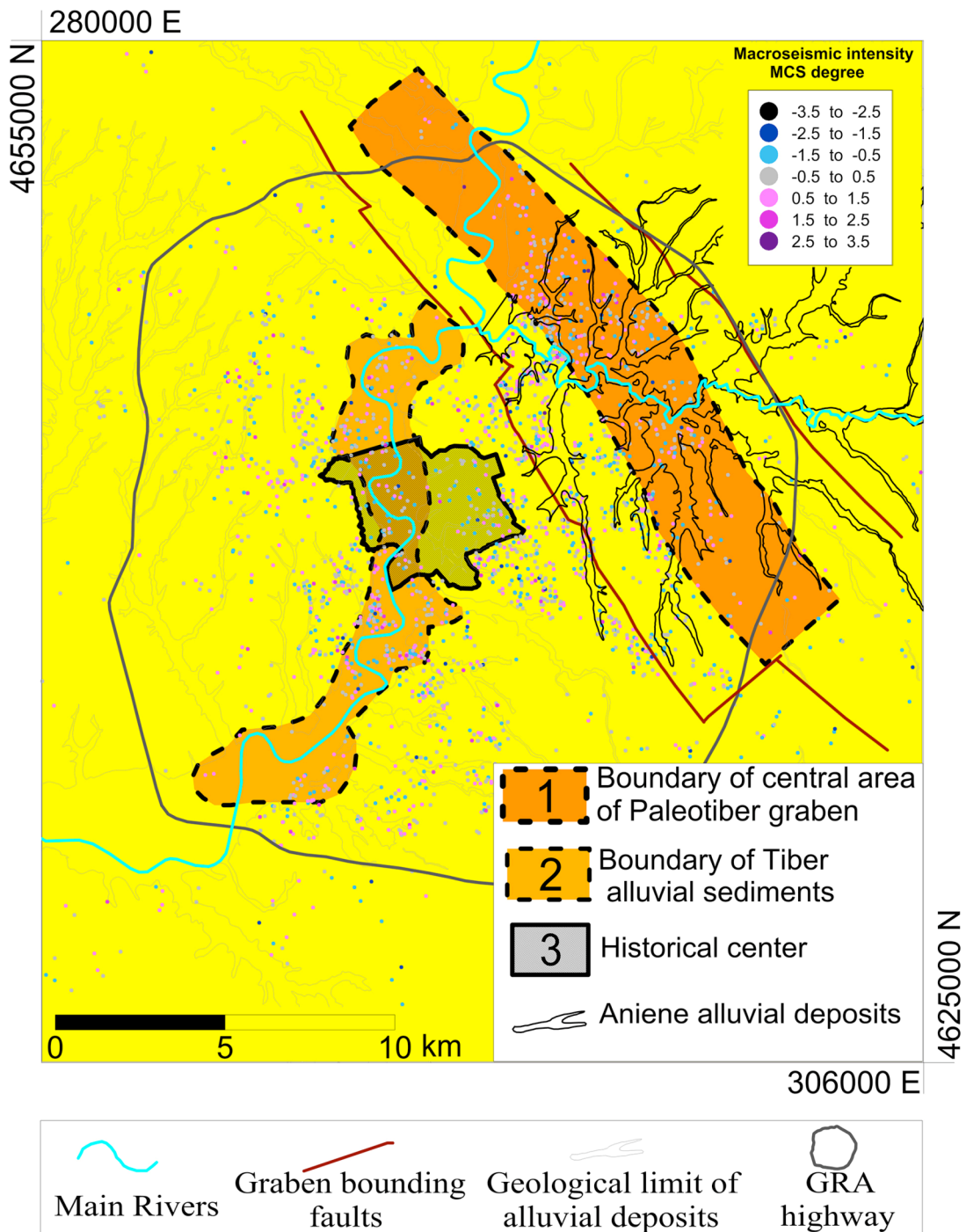


Figure 7

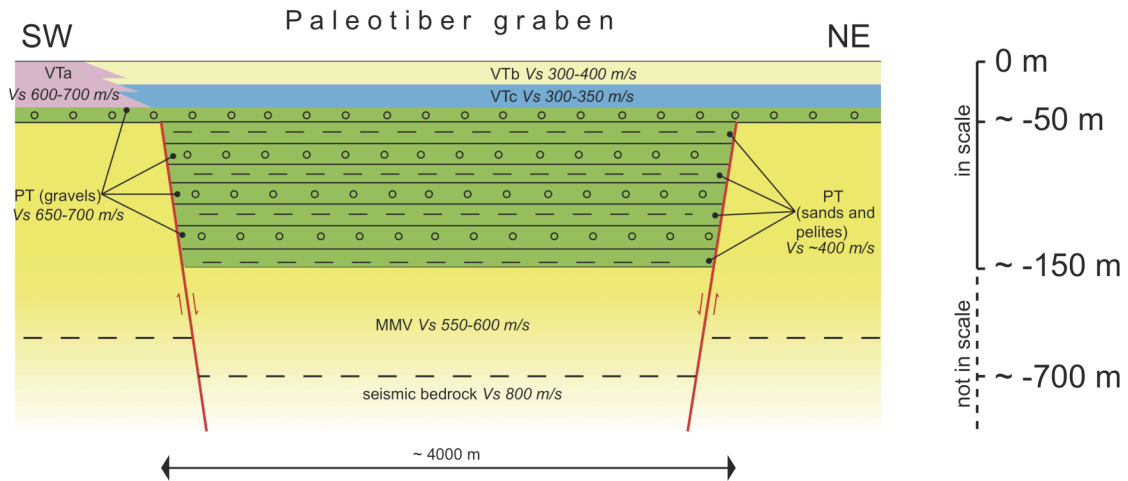


Figure 8

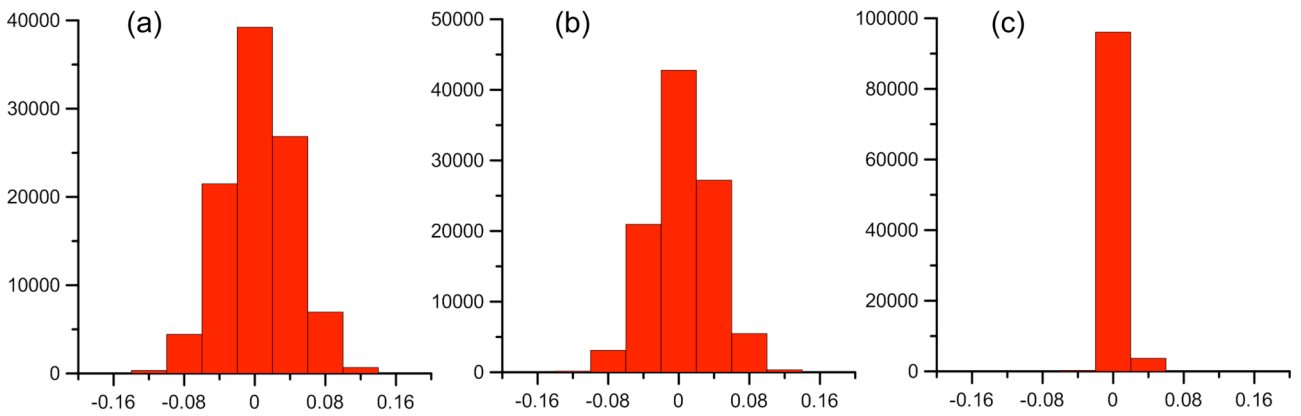


Figure 9

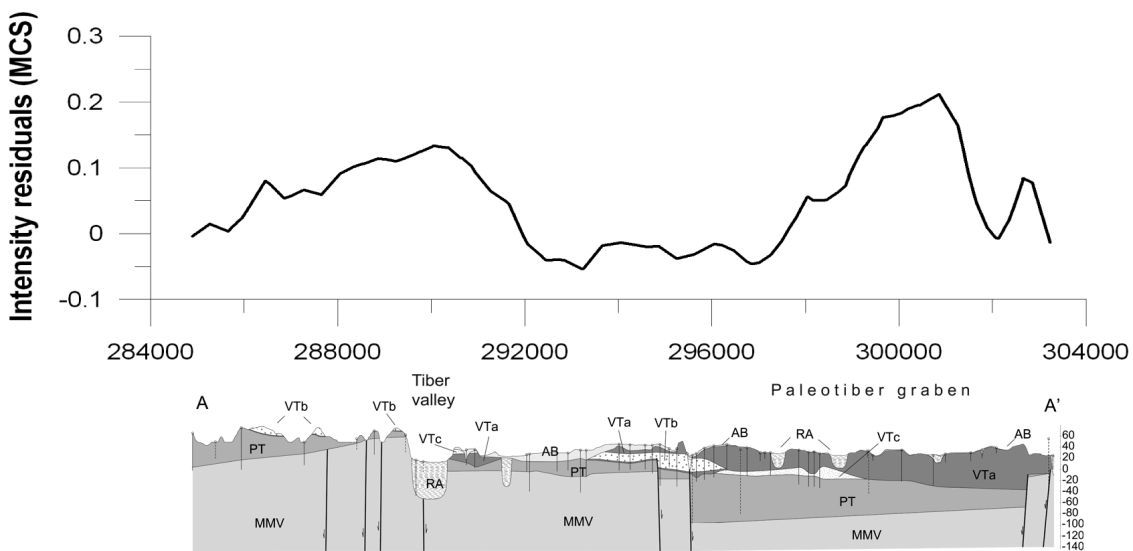


Figure 10

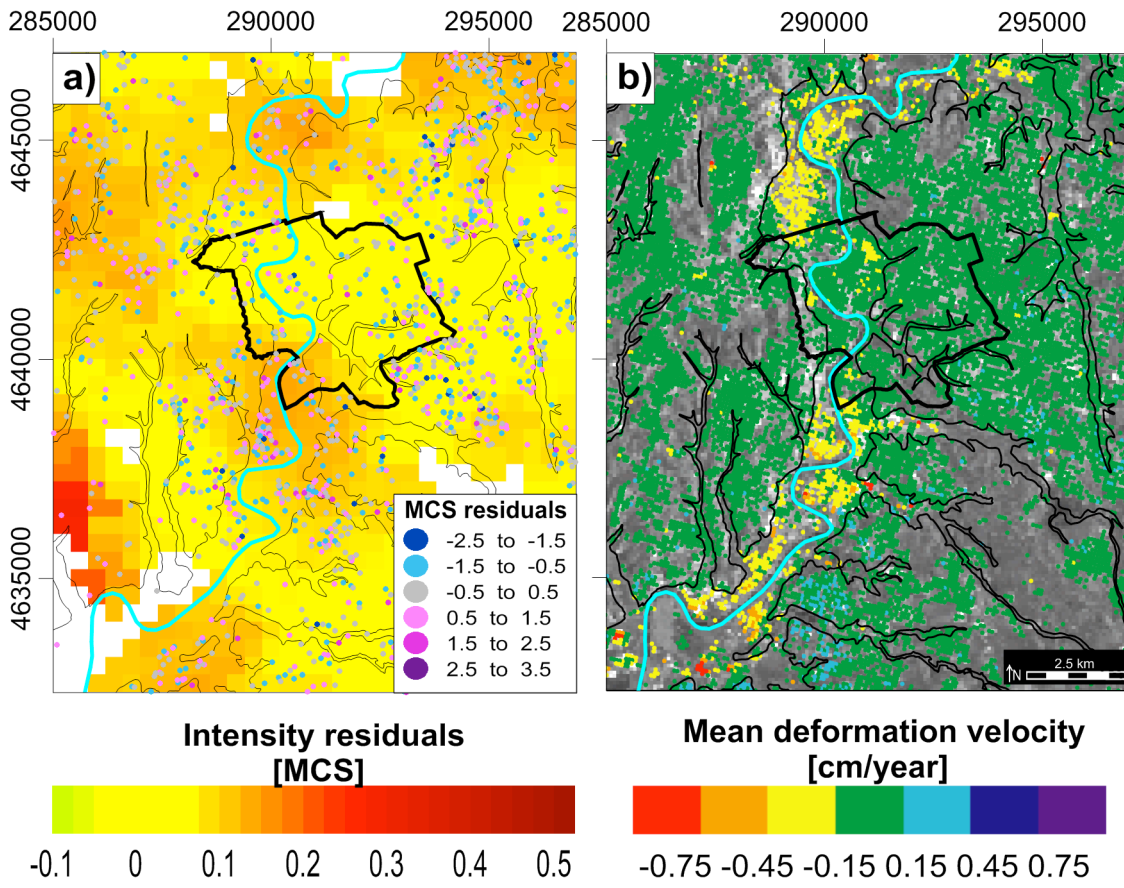


Figure 11